The effect of onboard passengers' seating arrangement on the vertical ride comfort of a high-speed railway vehicle

Mohammad Ali Rezvani[1,*], Robert Arcos[2], and Vahid Bokaeian[1,3]

[1]Center of Excellence in Railway Transportation, School of Railway Engineering, Iran University of Science and Technology, Tehran, Iran,

[2]Acoustical and Mechanical Engineering Laboratory, Universitat Politècnica de Catalunya, Spain,

[3]Acoustical and Mechanical Engineering Laboratory, Universitat Politècnica de Catalunya, Spain.

*Corresponding author: Mohammad Ali Rezvani, Email: rezvani_ma@iust.ac.ir

Abstract

This research is concerned with the impact of onboard passengers' seating arrangement on the carbody flexural vibrations of a high-speed railway vehicle. In this regard, the previously developed passenger body-seat models are used to consider the dynamic influence of the passengers. The carbody is modeled using the Euler-Bernoulli beam model to evaluate its flexural deformation. The frequency-domain analysis demonstrates that the carbody behaves almost like a rigid body when the vehicle is full of passengers. It is established that the passengers' presence causes a 31 percent enhancement of the ride quality determined based on EN 12299 standard for a fully occupied vehicle compared with an empty car. A scaled model of a ratio of 1:24.5 of the Shinkansen vehicle is constructed for validation purposes. The experimental results exhibit a similar trend as found by the simulations in terms of the impact of the passengers' distribution on the carbody flexural vibrations.

Keywords: Passenger body-seat dynamic; Flexural vibrations of carbody; Random vibration; Rail vehicle dynamics; Ride quality index.

1. Introduction

Railway vehicle dynamic behavior is significantly influenced by its carbody bending flexural modes, especially the first one. In this regard, a considerable size of fairly recent research has been reported. Zhou et al. (2009)[1] considered the impact of carbody elastic vibrations on passenger comfort of the railway vehicle. Also, they discussed the geometric filtering effect and its effect on the flexural vibrations of the carbody. Younesian et al. (2014)[2] investigated the influence of flexible carbody on the dynamic behavior of high-speed trains moving on bridges. Their study concluded that, in these cases, the flexural modes of the carbody significantly influence ride comfort, particularly in the range of low-frequency. Shi and Wu (2016)[3] analyzed the carbody's flexural vibration of the high-speed EMU. They indicated that the lowest natural frequency of the carbody is considerably close to the bogie's hunting frequency. Qi et al. (2018)[4] studied the effect of ballast bed and track irregularity on the vertical vibrations of carbody with considering its flexibility. Ling et al. (2018)[5] proposed a 3D model to investigate the carbody flexural vibrations of high-speed vehicles. They combined the multi-body dynamic, and finite element approaches for modeling the rigid motions and elastic deformation, respectively. Bokaeian et al. (2019 & 2020)[6, 7] carried out separate investigations on the effect of carbody flexibility in the Shinkansen high-speed train ride quality. Yan et al. (2021)[8] studied the impact of Maglev carbody flexibility on its vertical vibrations. They concluded that flexible carbody illustrated more significant vibration when compared with the rigid carbody because of flexural mode shapes of the elastic carbody. Pandey (2021)[9] investigated the influence of elastic deformation of freight carbody on its dynamic behavior. He reported a 40% increase in lateral acceleration when the carbody is considered flexible.

Deng and Chen (2021)[10] conducted a running test to measure the bogie frame and carbody vibrations. The measured results demonstrated an interaction between these vibrations. Those studies, through simulations, proved that when considering the carbody's flexibility, the first mode of its bending deformation has the most crucial effect on the ride quality. However, the torsional vibrations also prove stimulus for the passenger seated near the carbody wall, while this effect is smaller than the one related to the first bending mode. On the other hand, extensive studies to reduce the carbody flexible vibrations are executed by several researchers. Sugahara et al. (2008)[11] implemented a method to reduce the flexural and rigid vibrations by damping control of the primary suspension and also air spring, respectively. Takigami and Tomioka (2008)[12] utilized two different shunt circuits to suppress the carbody bending vibrations. Their experimental measurements established a 30% enhancement. Tomioka and Takigami (2010)[13] proposed using the bogie frames as dynamic vibration absorbers to cancel the carbody bending vibrations. They demonstrated a dynamic interaction between the longitudinal movement of bogie frames and bending deflection of the carbody via the bogie-carbody connection in the longitudinal direction. Gong et al. (2012)[14] investigated the geometric filtering phenomenon consisting of the 'wheelbase filtering' and the 'bogie base filtering' effects of a railway vehicle. Also, they suggested mitigating the vertical vibration of the carbody through the application of DVAs. Huang et al. (2018)[15] studied the effect of equipment installed under the carbody on flexural vibration. They proved that the mounted equipment behaves like a dynamic vibration absorber. They reduced the flexural vibrations by optimizing the equipment's stiffness, damping, mass, and mounting position. Wang et al. (2019)[16] proposed to use active suspension with control delay to improve the ride comfort of road vehicles. Gong et al. (2019)[17] reported a problem of feet numbness induced by the floor vibration of a high-speed train. They reduced the carbody floor vibration by optimizing the elastic supports of the under-chassis equipment. Bokaeian et al. (2020)[18] used Tomioka and Takigami's idea (bogie-carbody dynamic interaction) to reduce the bending flexural vibrations of the carbody, while they assumed the traction rod as a nonlinear element. Chen et al. (2020)[19] proposed to apply dynamic optimization of the suspension parameters of mounted equipment under the carbody chassis. Fu and Bruni (2021)[20] utilized four different active and semi-active configurations for primary and secondary suspension systems, including LQG and H_∞ control methods. They established that active secondary suspension has the best performance for reducing the rigid and flexible vibrations, simultaneously. Huang and Zeng (2021)[21] eliminated the elastic vibration of carbody that arises from the bogie frame by utilizing a hanged dynamic vibration absorber from the bogie frame. Investigations carried out by Nagai et al. (2006)[22], Tomioka and Takigami (2015)[23], and Tomioka et al. (2017)[24], among others, have found that passengers can serve, somehow, as dynamic vibration absorbers. Nagai et al. (2006)[22] modeled the passenger's dynamic by one degree of freedom. They concluded that the passengers' dynamic suppresses the first bending mode of the carbody. Tomioka and Takigami (2015)[23] studied the effects of numbers, postures, and arrangement of passengers on the flexural vibration of the carbody. They demonstrated experimentally and numerically that when the passengers exist on the vehicle, a large part of the peak value of acceleration PSD is canceled; therefore, they concluded that the passengers act as damper elements. Yu et al. (2020)[25] proposed a comprehensive model that included passengers, vehicles, and track models to investigate the vertical vibrations of the passengers. Such works proposed different passenger body-seat dynamic models to consider the coupled flexural vibrations of the carbody and its passengers. Therefore, it is vital to investigate the influence of the passengers on the carbody vertical vibrations and the consequences to the vehicle's ride comfort through a comprehensive dynamic model.

The prime purpose of this research is to examine the effect of passengers' dynamics and seating arrangement on the vertical ride comfort of the railway vehicle. The proposed models by

Nagai[22] and Tomioka and Takigami[23] are used to model passenger body-seat dynamics. As a novelty to this research, the effect of onboard passengers' distribution on the Shinkansen rail vehicle ride comfort is investigated by considering two significant cases, including the symmetric and asymmetric distribution of onboard passengers. In contrast, in previous studies, the passengers were distributed symmetrically. In addition, the impact of the system's natural frequency and damping ratio on the carbody's vertical acceleration and ride comfort that was noted in prior research are investigated.

Furthermore, the carbody is assumed as an Euler-Bernoulli beam with the free-free boundary conditions under vertical forces from the secondary suspension. The results obtained through both proposed passenger body-seat models are compared. Also, a replica of the Shinkansen rail vehicle at a scale of 1:24.5 is used to study the effect of passengers' seating arrangement onboard the vehicle on the bending flexural vibrations of the carbody, hence on its ride comfort.

2. Numerical studies of the full-scale vehicle

2.1 Model of the vehicle for vertical motion

Figure 1 schematically illustrates the railway vehicle's vertical motion model, including passengers' seats. The rigid degrees of freedom for carbody and bogie frames are the bounce and pitch and the bounce for the wheelsets.

Also, the carbody is modeled by using a simple uniform Euler-Bernoulli beam with the free-free boundary condition to study its flexural vibrations. Besides, the normal contact forces between wheelsets and rail are modeled with the linearized Hertzian theory.

The passenger-seat model is considered as a dynamic system with one degree of freedom that consists of a mass m_p, stiffness k_1, and damping c_1. This model was introduced by Nagai et al.[22]. They executed an experimental test to obtain the accelerance FRF between the passenger's chest and the seat. Then they identified the natural frequency and damping ratio and calculated the stiffness and damping coefficients through the following equations.

$$k_1 = 4\pi^2 m_p f_1^{\,2} \tag{1}$$

$$c_1 = 2\eta_1 \sqrt{m_p k_1} \tag{2}$$

Later on, Tomioka and Takigami[23], through a separate experimental test, identified different values for the natural frequency and damping ratio of the passenger-seat model. Indeed, the identification method they used was different from the method utilized by Nagai et al.

The present study uses the model for the dynamic system with one degree of freedom proposed by Nagai et al. [22] and Tomioka and Takigami[23]. The identified natural frequencies and damping ratios by Tomioka and Takigami and Nagai et al. are listed in Table 1.

Table 1. The parameters of the passenger body-seat dynamic model[22, 23].

The proposed model	symbol	value
By Nagai et al.[22]	f_1	5.5 Hz
	η_1	0.24 (%)
By Tomioka and Takigami[23]	f_1	7 Hz
	η_1	0.40 (%)

By considering the carbody as an Euler-Bernoulli beam, the dynamic vehicle equations of motion can be formulated as follow.

Carbody's equations of motion[6]:

$$\ddot{\imath} + \xi\omega\dot{} + \omega = \frac{1}{m_c}\left[-f_{sf}Y_n(l_f) - f_{sr}Y_n(l_r) + \sum_{i=j}^{k}\left(k_1\left[z_{pi} - z_c(l_i,t)\right] + c_1\left[\dot{z} - \dot{} \right]_{,} {}_n(l_i)\right]\right. \tag{3}$$

$$\omega_n^2 = \beta_n^4\frac{EI}{\rho A},\quad 2\zeta_n\omega_n = \beta_n^4\frac{\mu I}{\rho A}$$

$$m_c\ddot{} = - \quad -f_{sr} + \sum_{i=j}^{k}\left(k_1\left[z_{pi} - z_c(l_i,t)\right] + c_1\left[\dot{z} - \dot{} \right]_{,}\right. \tag{4}$$

$$I_c\ddot{\theta}_{} = {}_{,} - l_b f_{sr} - \sum_{i=j}^{k}\left(k_1 l_i\left[z_{pi} - z_c(l_i,t)\right] + c_1 l_i\left[\dot{z} - \dot{} \right]_{,}\right. \tag{5}$$

$$\begin{aligned} m_p\ddot{} = \quad & \left[z_{pi} - \left\{z_c + \left(\frac{l}{2} - l_{pi}\right)\theta_c + Y_1(l_{pi})q_1\right\}\right] \\ & -c_1\left[\dot{z} - \left\{\dot{} + \left(\quad - \quad\right)\dot{\theta}_{} + \quad\right\}\right] \quad = 1,2,...,18 \end{aligned} \tag{6}$$

where $Y_n(x)$, f_{sf} and f_{sr} are the shape functions of the carbody bending and the front and rear secondary suspension forces in the vertical direction. They are defined as[6]

$$\mathrm{Y_n(x)} = \mathrm{ch}\,\beta_n\mathrm{x} + \cos\beta_n\mathrm{x} - \frac{\mathrm{ch}\beta_n\mathrm{l} - \cos\beta_n\mathrm{l}}{\mathrm{sh}\,\beta_n\mathrm{l} - \sin\beta_n\mathrm{l}} \times (\mathrm{sh}\,\beta_n\mathrm{x} + \sin\beta_n\mathrm{x}) \tag{7}$$

$$f_{si} = c_s[\dot{z} \quad - \dot{} \quad + \quad {}_i,t) - z_{bi}],\ i = f,r \tag{8}$$

$$z_c(x,t) = z_{cr}(t) + (\frac{l}{2} - x)\theta_c(t) + z_{cf}(x,t) \tag{9}$$

while $z_c(x,t)$ is the carbody vertical motion at position x and time t, including rigid (z_{cr}, θ_c) and flexural (z_{cf}) motions. Also, k_1 and c_1 are stiffness and damping coefficient of passenger body-seat dynamic model, respectively.

The ith bogie frame and its wheelsets' equations of motion are[6]:

$$m_b\ddot{} \quad -f_{pif} - f_{pir},\ i = f,r \tag{10}$$

$$I_b\ddot{\theta}_{} = {}_{} - f_{pif} - l_w f_{pir},\ i = f,r \tag{11}$$

$$m_w\ddot{} = {}_{} - N_{wif},\ i = f,r \tag{12}$$

$$m_w\ddot{} \quad - \quad = \tag{13}$$

In equations (10) to (13), the sub-indexes f and r correspond to the front and rear bogie, respectively, while f_{pif} and f_{pir} are vertical forces of the primary suspension in the front and rear bogies, respectively, and N_{wij} is the normal contact force between jth wheelset of the ith bogie and the rail. The related definitions are[6]:

$$\begin{aligned} f_{pif} &= c_p[(\dot{z} \quad - \quad \theta \quad - \dot{} \quad + \quad - l_w\theta_{bi}) - z_{wif}] \\ f_{pir} &= c_p[(\dot{z} \quad + \quad \theta \quad - \dot{} \quad + \quad + l_w\theta_{bi}) - z_{wir}] \end{aligned} \tag{14}$$

$$N_{wij} = k_{hz}\delta_{wij},\quad \delta_{wij} = z_{wij} - z_{0ij} \tag{15}$$

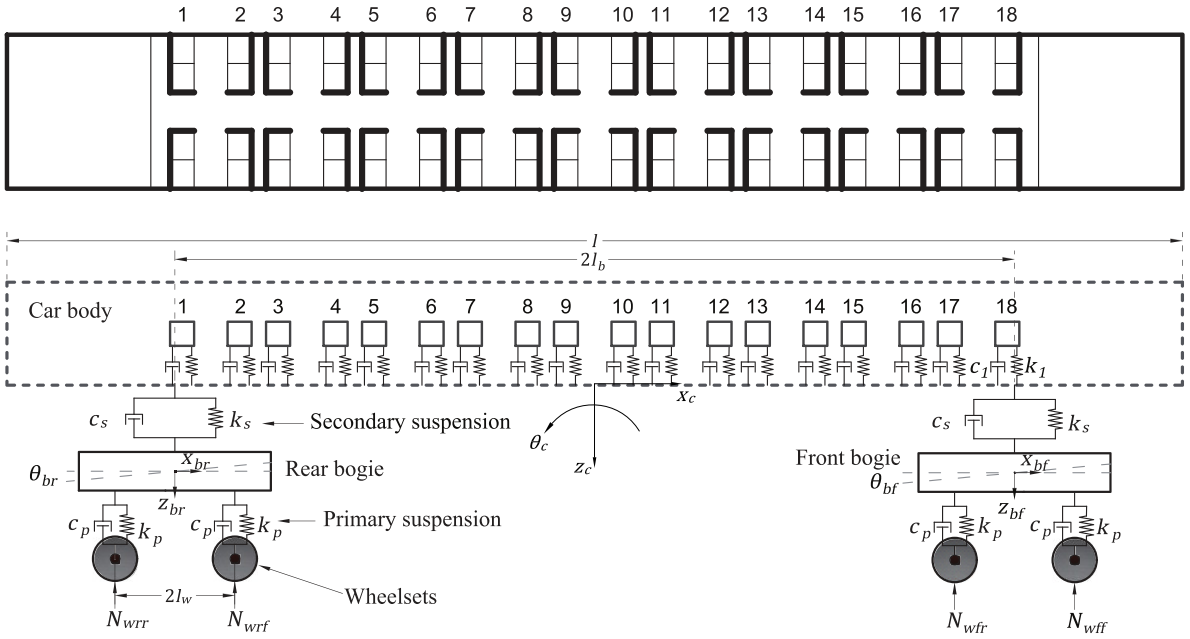

Figure 1. A vertical model of the Shinkansen vehicle (series 100). Numbers on the passengers' models refer to their corresponding row number.

The other physical and mechanical characteristics of the Shinkansen vehicle considered in this research are listed and defined in Table A.1 of Appendix A.

2.2 Track irregularity

To comply with the suggested degrees of freedom for the vehicle (vertical and pitch rigid and bending flexural motions), the only source of the model excitation is the track vertical irregularity. Since no measurement was taken to represent the actual rail track vertical irregularity, the power spectral density of German low irregularity, matched with the vehicle running speed (300 km/h), is used in this research, as follows[26].

$$S_v(\Omega) = \frac{A_v\,\Omega_c^2}{\left(\Omega^2+\Omega_r^2\right)\left(\Omega^2+\Omega_c^2\right)} \tag{16}$$

while $S(\Omega)$ is the power spectral density of track vertical irregularity in spatial frequency domain. Ω is spatial frequency, λ (m) is the wavelength of the track irregularity, therefore, $\Omega = 1/\lambda\,(\mathrm{rad/m})$. A_v is roughness constant and equal to 4.032×10^{-7} $(\mathrm{m.rad})$ Ω_c and Ω_r are cutoff spatial frequency; these constants are equal to 0.8246 (rad/m), 0.0206 (rad/m), respectively. On the vehicle wheel, this irregularity in the frequency domain, at the running speed of v (m/s), can be accounted for by using equation (17)[6].

$$S(\omega) = \frac{S_\Omega\left(\omega/v\right)}{v} \tag{17}$$

3. The scaled experimental model of the vehicle

A 1:24.5 experimental scaled model of the Shinkansen vehicle was set up to investigate the impact of passengers' seating arrangement on the flexural vibration of the carbody. The passengers' seating arrangement onboard the vehicle is also represented by defining the passengers' center of gravity along the longitudinal direction, as presented in Figure 2.

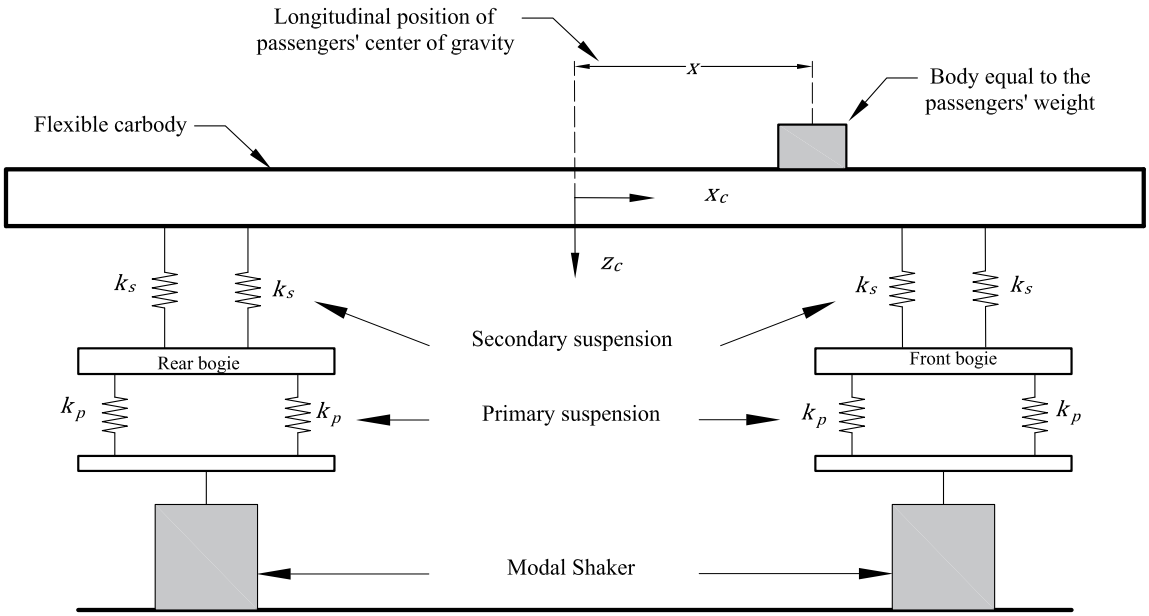

Figure 2. Schematic view of the constructed scaled model.

The constructed model is excited by the simultaneous use of two modal shakers (Sinocera-JZK-20). Due to the limited equipment, the scaled model in this research is built to represent a 2-axle vehicle. Therefore, within the scald model, the effect of pitching of bogie frame on the vertical acceleration of carbody can not be detected. In this regard, the German low irregularity profile is generated using a laptop. Then the generated digital data of the irregularity is converted to analog signals through a DAC (Digital to Analog Converter) card (BMCM-AD16f). Two separate amplifiers (Sinocera-YE5873A) were used to amplify the analog output from the converter card before they were delivered to the modal shakers. The results of the test are measured by triaxial accelerometers (Sinocera-CA-DR-3001). The mass of the accelerometer is 30 gr, which is equivalent to the scaled mass of six passengers sated on the carbody center. However, the passengers' distribution is defined based on the longitudinal distance between the passengers' center of gravity and the carbody center. Therefore, the effect of the accelerometer mass on the system dynamics can be ignored.

The technical specifications related to the modal shakers and accelerometers are listed in Tables 2 and 3.

Table 2. Technical specifications of the modal shakers.

Model	JZK-20
Type	Piezotronic
Max. peak force, sin/random	200/140 N
Max. travel	±5 mm
Max. acceleration	400 m/s^2
Effective moving mass	0.5 kg
Frequency range	2 Hz to4000 Hz
Provider	Sinocera/China

Table 3. Technical specifications of the accelerometers.

Accelerometer	CA-DR-3001
Type	Triaxial capacitance
Mass	30 gr
Measurement range (peak value)	±50g m/s^2
Frequency range	1 Hz to 5000 Hz
Max noise	0.4 mg
Axial sensitivity	100 mV/g
Max transverse sensitivity	5 %
Provider	Sinocera/China

3.1 The scaling methodology

The method for scaling in the present research is based on the scheme of inspectional analysis, which is highly dependent on the understanding of system motion equations. By defining the length ($\varphi_l = l_1/l_0$ where l_0 and l_1 are the lengths of the scaled and the full scale model, respectively) and time ($\varphi_t = t_1/t_0$) scale factor, the other scaling factors can be calculated as listed in Table 4.

Table 4. The scaling factors of the similarity law[27].

Scaling factor	Equation
Cross-section	$\varphi_A = \varphi_l^2$
Volume	$\varphi_V = \varphi_l^3$
Velocity	$\varphi_v = \varphi_l / \varphi_t$
Acceleration	$\varphi_a = \varphi_l / \varphi_t^2$
Density	$\varphi_\rho = \rho_1 / \rho_0$
Mass	$\varphi_m = \varphi_\rho \varphi_l^3$
Moment of inertia	$\varphi_I = \varphi_m \varphi_l^2$
Force	$\varphi_F = \varphi_\rho \varphi_l^4 / \varphi_t^2$
Stiffness	$\varphi_k = \varphi_\rho \varphi_l^3 / \varphi_t^2$

Based on this strategy, as the dynamic studies are performed in the time and frequency domains, the scaling factor of the time and, consequently, the scaling factor of the frequency is equal to unity. Because of the equipment limitation and also the scope of the experiment, which focuses on the effect of passengers' seating arrangement on carbody flexural vibrations, the length scale factor is chosen as follows

$$\varphi_l = 24.5 \tag{18}$$

Within the dynamic analysis framework, the most significant variables to consider are the bodies' displacement, velocity, and acceleration and the forces that interact between the bodies. With the above definitions, the scaling factor results in:

$$\text{For displacement } \varphi_l = 24.5 \tag{19}$$

$$\text{For velocity } \varphi_v = 24.5, \tag{20}$$

$$\text{For acceleration } \varphi_a = 24.5, \tag{21}$$

Therefore, the characteristics of the full scale and the scaled models are listed in Table 5. The damping effect of the primary and the secondary suspensions is not considered.

Table 5. Characteristics of the original and the scaled models.

Parameter	Full-scale	Scaled
Carbody mass (kg)	16900	1.149
Bogie frame mass (kg)	2580	0.175
Passenger mass (kg)	75	0.005
Carbody length (m)	24.5	1
Bogie-base (m)	17.5	0.7143
Wheel-base (m)	2.5	0.102
Primary vertical stiffness (N/m)	19700000	1339
Secondary vertical stiffness (N/m)	2560000	174.1

3.2 Scaled experimental results

To study the effect of the onboard passengers' seating arrangement on the vehicle dynamic, four different scenarios that are presented in Figure 3 are considered. These include:

- Case 1: There are no passengers onboard the vehicle. Therefore, the center of gravity is located at the carbody center.
- Case 2: There are 20 passengers onboard the vehicle. The seating arrangement is such that the center of gravity of the passengers is 10 cm away from the carbody center along the carbody centerline. The total scaled mass of the passengers is equal to 100 gr. The scaled mass of the individual passengers is equal to 5 gr.
- Case 3: Same as in case 2, there are 20 passengers onboard the vehicle. The seating arrangement is such that the center of gravity of the passengers is 18 cm away from the carbody center along the carbody centerline. The total scaled mass of the passengers is equal to 100 gr.
- Case 4: It is assumed that there are 40 passengers onboard the vehicle. The seating arrangement is such that the center of gravity of the passengers is 10 cm away from the carbody center along the carbody centerline. The total scaled mass of the passengers is equal to 200 gr.

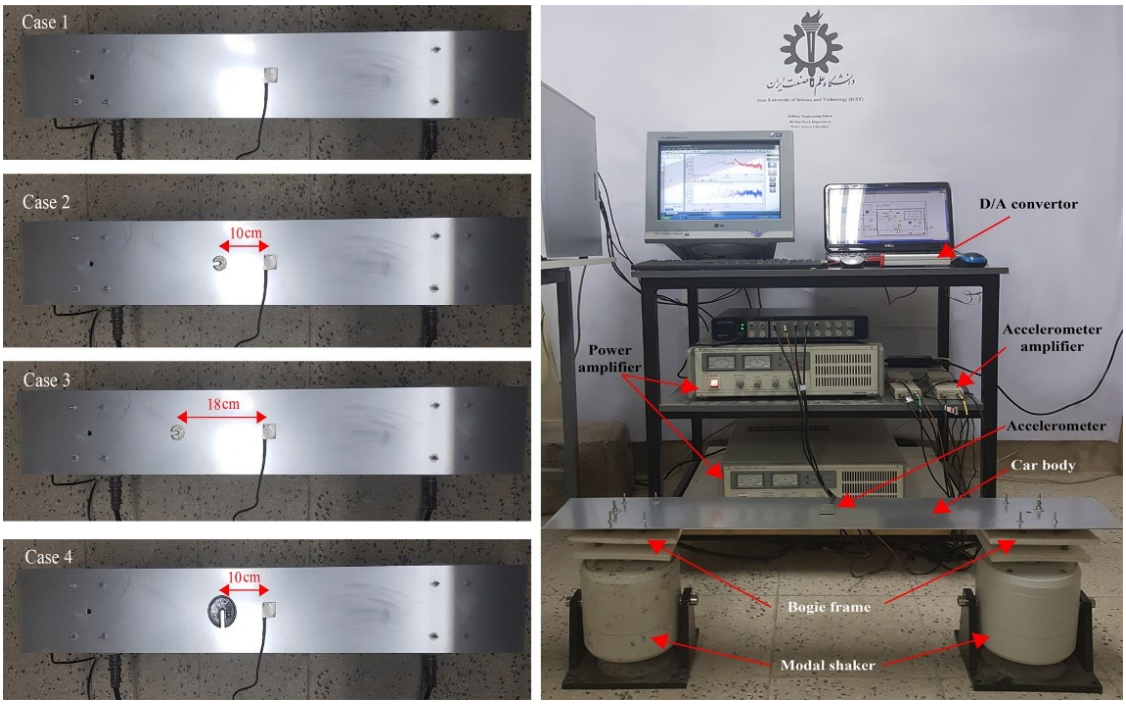

Figure 3. The test setup of the scaled vehicle. The scaled model (right) and the passengers' distribution scenarios (left).

Figure 4 compares the vertical acceleration PSD at the carbody center from the numerical simulation of the scaled vehicle for the four cases of the onboard passengers' seating arrangement. Also, in Figure 5, the simulation and the measured results for the scaled model are compared for the four previous cases. Figures 4 and 5 show three considerable peaks in the vertical acceleration PSD at the carbody center. The peaks occurring at frequencies of 1 Hz and 5 Hz mainly correspond to the vertical and pitch motion of the carbody, respectively. The resonant peak at 10 Hz is related to the first mode of carbody bending. Figure 5(a) results correspond to an empty vehicle; in this scenario, this resonant peak at 10 Hz appears in the vertical acceleration PSD. In scenarios 2 to 4, with the passengers occupying the vehicle, the passengers' dynamic behavior partially canceled this resonant peak relevant to the first mode of carbody bending, as presented in Figures 5(b) to 5(d).

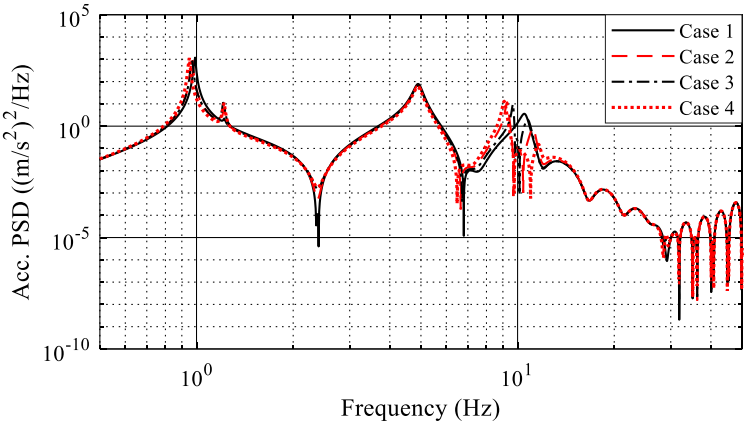

Figure 4. The predictions by the numerical simulation for the effects of the onboard passengers' seating arrangement on the vertical acceleration of the carbody center of the scaled vehicle.

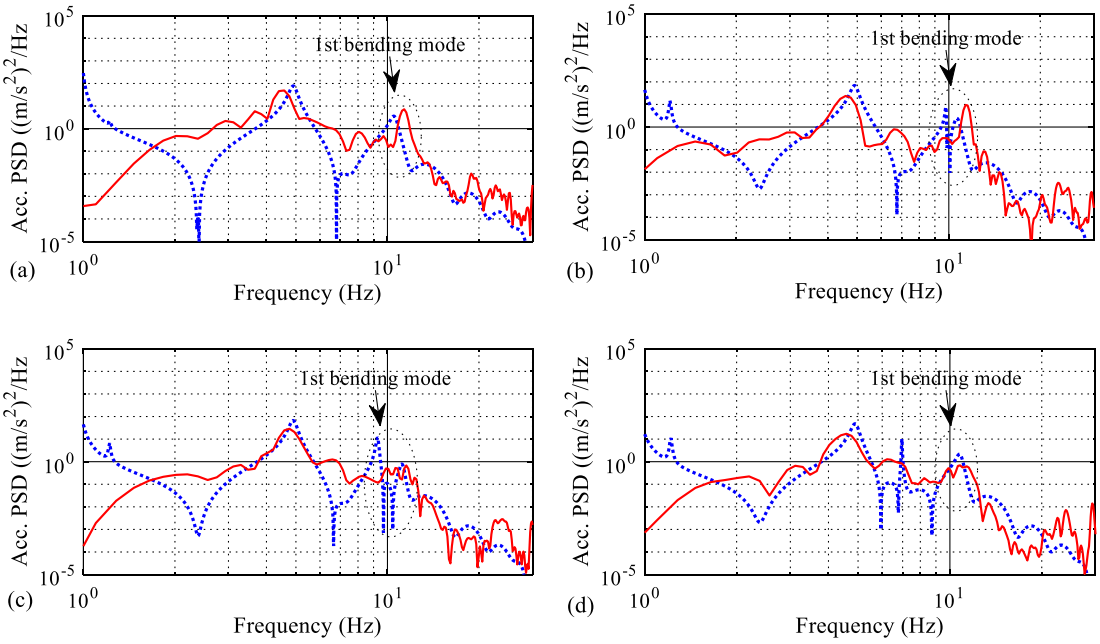

Figure 5. Comparison between the simulation (blue) and the measured (red) results of the onboard passengers' seating arrangement effect on the carbody first bending mode for the scaled vehicle. a) case 1, b) case 2, c) case 3, and d) case 4.

4. Simulation and analytical results

4.1 Full-scale model verification

In this subsection, the results obtained through simulation for the Shinkansen high-speed rail vehicle for running speed of 300 km/h are compared with the measurements from the field tests for the same vehicle executed by Tomioka Takigami[13]. Figure 6 demonstrates the vertical acceleration at the carbody center for the simulation and running tests in the frequency domain. Between two sets of results, there is a good agreement for the outcome at a frequency of about 10 Hz, where the natural frequency of the first bending mode is located. When concerned with the ride quality, it is known that the carbody first bending mode is the most important factor for measuring PSD of the vertical acceleration. Before estimating the ride comfort, the acceleration response needs to be weighted by applying a band-pass filter, which allows the passage of signals in the frequency range of 4 to 20 Hz and attenuates the signals outside this frequency band. From the results in Figure 6 (b), the ride comfort level is almost determined by the component of the acceleration response around 10 Hz (the carbody first bending mode). In contrast, for the other frequencies, the acceleration effect is ignorable. There is a decent agreement between the simulation and the measured results around the carbody's first bending mode.

It is also noted that some anti-resonances appeared periodically in the simulation results. Such anti-resonances occur at the frequencies where the total effect of the vertical excitation to the system disappears. These are the wheel-base and bogie-base filtering frequencies (Bokaeian et al. (2019)[7]).

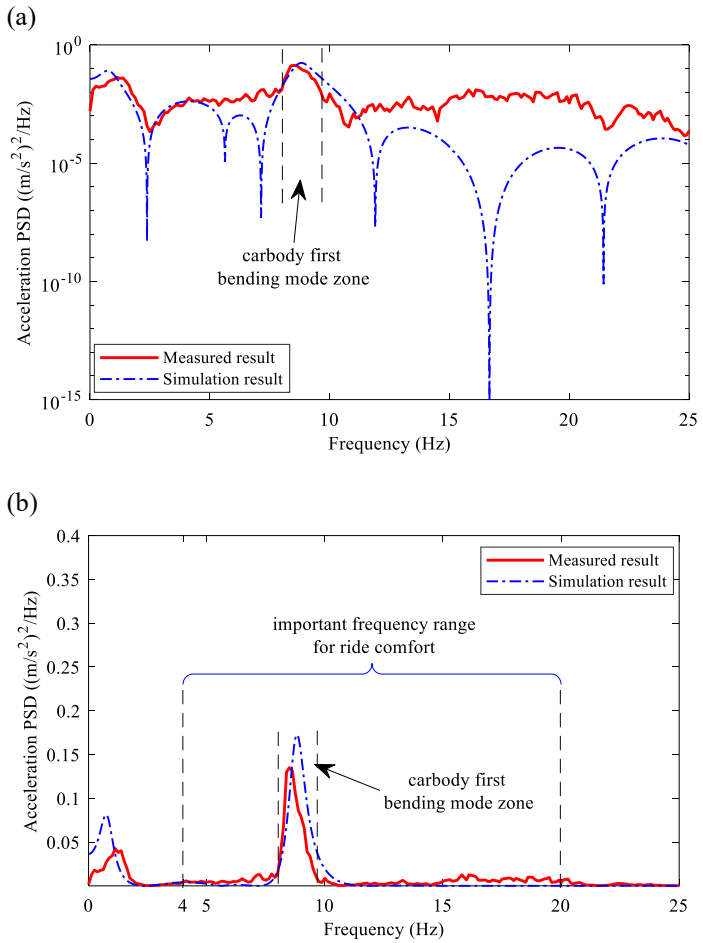

Figure 6. Comparison of the simulation and the measured results[13] for the vertical acceleration at the carbody center of the Shinkansen vehicle series 100, a) Logarithmic and b) Linear scales.

4.2 Bending vibrations of the carbody

Figure 7 illustrates the effect of passengers' distribution on the contribution of the first mode to the carbody bending vibrations, using the passenger-vehicle Tomioka-Takigami's coupling model for the symmetrical and asymmetrical passengers' arrangement. When the passengers' distribution is symmetric, the passengers' center of gravity is located at the carbody center of gravity. For this case, denoting the arrangement presented in Figure 1, when rows 8 to 11 are occupied, 86.9 percent of the peak related to the first mode of bending on the vertical acceleration PSD at the carbody center is attenuated (peak value is decreased from 0.2179 $(m/s^2)^2/Hz$ to 0.0285 $(m/s^2)^2/Hz$). If all the rows are occupied, this attenuation is 94.2 percent (peak value is reduced from 0.2179 $(m/s^2)^2/Hz$ to 0.0125 $(m/s^2)^2/Hz$).

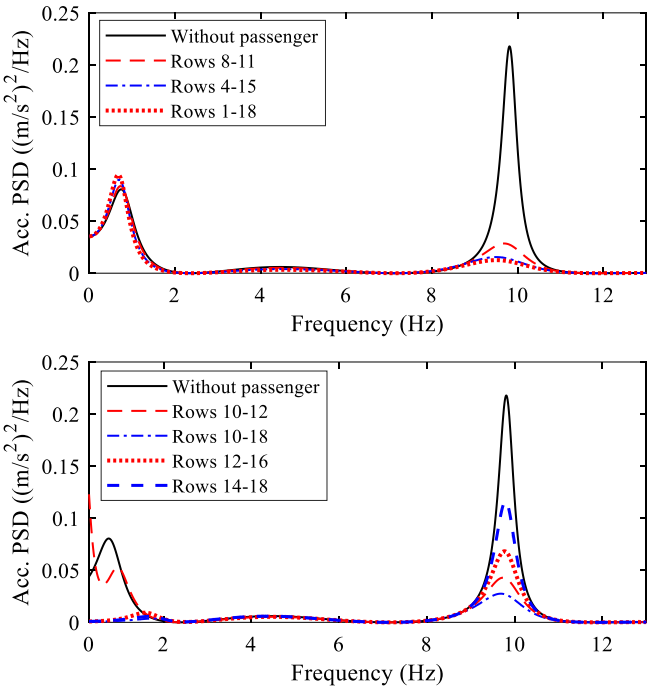

Figure 7. The effect of onboard passengers' distribution on the carbody's flexural vibrations; symmetrical (upper) and asymmetrical (lower) distribution.

The passengers' distribution is considered asymmetric when the passengers' canter of gravity is far from the carbody center of gravity in the longitudinal direction. In this case, when rows 10 to 18 are occupied, the peak related to the first mode of the carbody bending on its vertical acceleration PSD is canceled by 87.3 percent (peak value is decreased from 0.2179 $(m/s^2)^2/Hz$ to 0.0275 $(m/s^2)^2/Hz$). Indeed, when the passengers are in the vehicle, the passenger body-seat dynamic system acts as a dynamic vibration absorber (DVA) and cancels out part of the carbody's flexural vibrations. By comparing this set of results, it can be interpreted that for a fixed number of passengers, a more significant part of the flexural vibrations will be canceled if the passengers' center of gravity is closer to the carbody's center of gravity. The onboard passengers act as a dynamic vibration absorber (DVA) for the carbody. Also, the maximum amplitude of the first bending mode occurs in the carbody center. Therefore, if it is desired to attenuate the carbody's first bending mode deflection, the center of gravity of DVA needs to be placed at the carbody center.

Figure 8 illustrates the vertical acceleration experienced by the passengers seated on the 9^{th} row obtained through both suggested models by Tomioka-Takigami and Nagai. It is clear that when Nagai's model is used, the flexural vibrations felt by passengers are higher because the

proposed model by Tomioka-Takigami is stiffer than Nagai's one. Specifically, the natural frequency of the passenger body-seat system is closer to the carbody's first bending mode. It implies that a more significant part of the flexural vibrations is canceled when Tomioka-Takigami's model is used to model the passenger body-seat dynamic behavior. For example, when the passengers occupy rows 8 to 11, the peak value of the PSD acceleration sensed by the passengers is 0.04 $(m/s^2)^2/Hz$ and 0.08 $(m/s^2)^2/Hz$ for Tomioka-Takigami and Nagai's models, respectively.

Figures 7 and 8 show that the carbody acts almost like a rigid body when the vehicle is fully occupied. In this case, 98.4 percent of the peak related to the first bending mode due to the vertical acceleration at the carbody center is canceled.

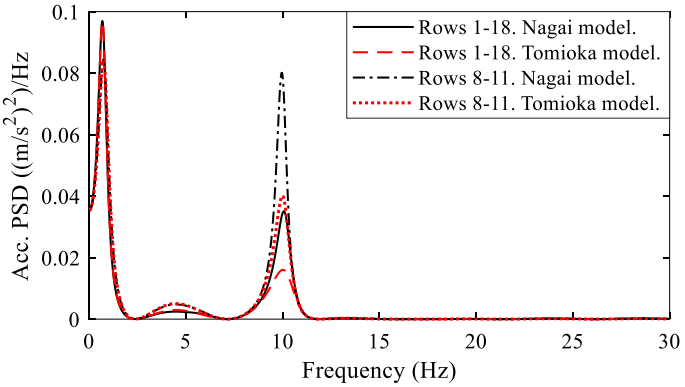

Figure 8. The vertical acceleration of the passenger seated on the 9th row according to Tomioka-Takigami and Nagai's models.

4.3 Ride quality evaluation

Figure 9 illustrates the impact of onboard passengers on the ride quality of the carbody center for the symmetric arrangement of the passengers' distribution. When rows 8 to 11 are occupied, and for the vehicle speed of 298.8 km/h, an improvement of 25.4 percent concerning the case of no passengers is observed (the ride quality index is 0.558 m/s^2). When passengers fully occupy the vehicle, the ride quality index improves by 36.6 percent. The reason for such an outcome was elaborated on in the previous subsection.

For the vehicle running speed under 220 km/h, the carbody behaves virtually as a rigid body. At these speeds, the first bending mode that appeared on the vertical acceleration of the carbody center is altogether canceled out. However, for a speed over 220 km/h, the carbody acts as a flexible body, influencing the ride quality. Also, the ride qualities for the rigid and flexible carbodies become closer to each other at some speed. This is due to the filtering frequencies related to the bogie and wheelbases. At these speeds, the anti-resonance frequencies are matched with the first bending mode of the carbody that causes cancelation of a significant part of the vibration mode.

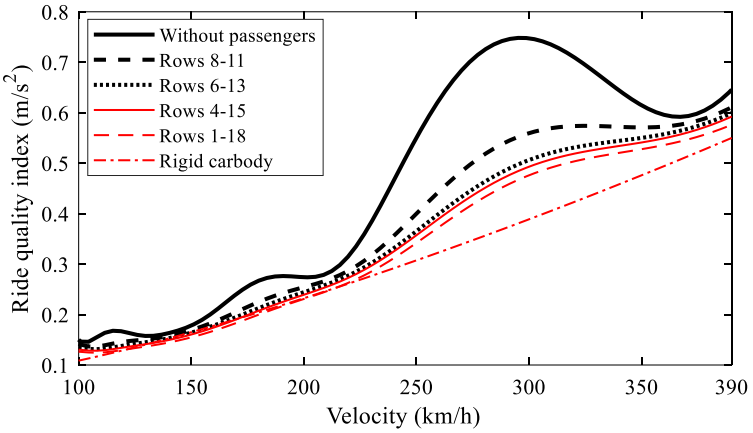

Figure 9. The estimated ride quality index at the carbody center for various onboard passengers' seating arrangements.

Figure 10 exhibits the ride quality index of the passenger seated on the 9th row obtained through Tomioka-Takigami and Nagai's proposed models. The ride quality index obtained by Nagai's model is higher than the one obtained through Tomioka-Takigami's model. The passenger-seat dynamic model's natural frequency and damping ratio can affect the numerical results for the vertical acceleration and, consequently, the ride quality.

For the case in which rows, 8 to 11 are occupied, and for the speed of 298.8 km/h, the estimated ride quality index by the Nagai's model is 10.22 percent higher than the one for the Tomioka-Takigami's model; the corresponding values are 0.626 m/s^2 and 0.562 m/s^2, respectively. A similar scenario occurs when all the rows are occupied, where the ride quality index obtained through Nagai's model is 10.84 percent higher than the one achieved by Tomioka-Takigami's model.

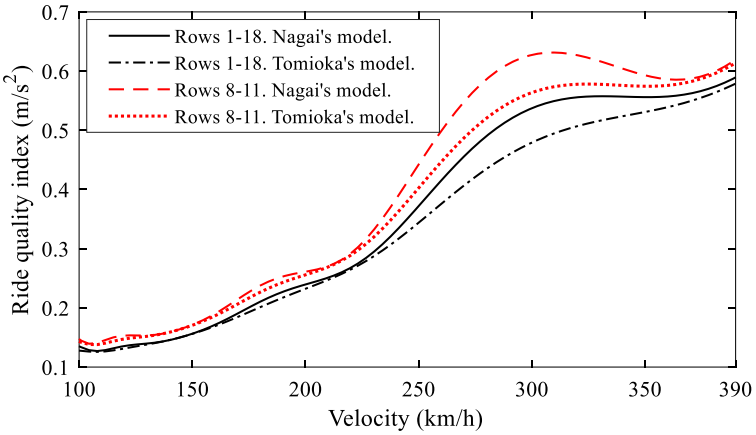

Figure 10. The estimated ride quality index for the passenger seated on the 9th row.

5. Conclusions

The present research is concerned with the effect of passengers' body dynamics on the rail vehicle's carbody flexural vibrations. The ride quality of a Shinkansen high-speed rail vehicle is examined by considering symmetric and asymmetric arrangements for the onboard seated passengers. The carbody is regarded as an Euler-Bernoulli beam. Tomioka-Takigami and Nagai's proposed models are used to investigate the passenger body-seat dynamic impact on the carbody's flexural vibrations. The following results are achieved:

1. A more significant effect on the flexural vibrations is achieved when the passengers are distributed closer to the vehicle's center of gravity. For example, when rows 8 to 11 are full of passengers, 86.9 percent of the carbody's flexural vibrations are eliminated.
2. It is observed that when Tomioka-Takigami's model is used to consider the passenger body-seat dynamic, a more significant part of the carbody's flexural vibrations seems to have been attenuated. This is because the natural frequency of the proposed model by Tomioka-Takigami is closer to the first mode frequency of the carbody bending.
3. It is attested that when the vehicle is full of passengers, its flexural modes become less critical, implying an approximated rigid body motion.

Acknowledgments

The authors would thank Professor Takahiro Tomioka for sharing treasured comments during this research. The second author wishes to appreciate further the financial support provided by the VIBWAY project, with reference RTI2018-096819-B-I00, financed via the Ministerio de Ciencia e Innovación, Retos de Investigación 2018.

Declaration of Conflicting Interests

The author(s) declared no potential conflicts of interest concerning this article's research, authorship, and publication.

References

1. Zhou J, Goodall R, Ren L, et al. Influences of car body vertical flexibility on ride quality of passenger railway vehicles. *Proc Inst Mech Eng, Part F: J Rail Rapid Transit* 2009; 223: 461-471.
2. Younesian D, Marjani SR and Esmailzadeh E. Importance of flexural mode shapes in dynamic analysis of high-speed trains traveling on bridges. *J Vib Control* 2014; 20: 1565-1583.
3. Shi H and Wu P. Flexible vibration analysis for car body of high-speed EMU. *J Mech Sci Technol* 2016; 30: 55-66.
4. Qi F, Lei Y, Deng P, et al. Car body vertical vibration analysis under track medium wave irregularity and the influence factors of ballast bed. *J Low Freq Noise Vibr Act Control* 2019; 38: 1160-1177.
5. Ling L, Zhang Q, Xiao X, et al. Integration of car-body flexibility into train–track coupling system dynamics analysis. *Veh Syst Dyn* 2018; 56: 485-505.
6. Bokaeian V, Rezvani MA and Arcos R. Nonlinear impact of traction rod on the dynamics of a high-speed rail vehicle carbody. *J Mech Sci Technol* 2020; 34: 15.
7. Bokaeian V, Rezvani MA and Arcos R. The coupled effects of bending and torsional flexural modes of a high-speed train car body on its vertical ride quality. *Proc Inst Mech Eng, Part K: J Multi-body Dyn* 2019; 233: 979-993.
8. Yan Z, Zeng J, Zhang W, et al. Dynamic Simulation of Vibration Characteristics and Ride Quality of Superconducting EDS Train Considering Body with Flexibility. *IEEE Trans Appl Supercond* 2021; 31: 1-5.
9. Pandey M. Effect of carbody flexibility on the dynamic performance of an empty freight wagon. *Proc Inst Mech Eng, Part F: J Rail Rapid Transit* 2021. DOI: 10.1177/09544097211028679.
10. Deng H and Chen S. Experimental Analysis of the Car Body Suspended Equipment Vibration for High-speed Railway Vehicles. In: *J Phys Conf Ser* 2020, p.012064. IOP Publishing.
11. Sugahara Y, Kazato A, Takigami T, et al. Suppression of vertical vibration in railway vehicles by controlling the damping force of primary and secondary suspensions. *Q Rep RTRI* 2008. DOI: 10.2219/rtriqr.49.7.
12. Takigami T and Tomioka T. Bending vibration suppression of railway vehicle carbody with piezoelectric elements (experimental results of excitation tests with a commuter car). *J Mech Syst Transport Logist* 2008; 1: 111-121.
13. Tomioka T and Takigami T. Reduction of bending vibration in railway vehicle carbodies using carbody–bogie dynamic interaction. *Veh Syst Dyn* 2010; 48: 467-486.

14. Gong D, Zhou JS and Sun WJ. On the resonant vibration of a flexible railway car body and its suppression with a dynamic vibration absorber. *J Vib Control* 2012; 19: 649–657.
15. Huang C, Zeng J, Luo G, et al. Numerical and experimental studies on the car body flexible vibration reduction due to the effect of car body-mounted equipment. *Proc Inst Mech Eng, Part F: J Rail Rapid Transit* 2018; 232: 103-120.
16. Wang Q, Zeng J, Wei L, et al. Carbody vibrations of high-speed train caused by dynamic unbalance of underframe suspended equipment. *Adv Mech Eng* 2018. DOI: 10.1177/1687814018818969.
17. Gong D, Wang K, Duan Y, et al. Car body floor vibration of high-speed railway vehicles and its reduction. *J Low Freq Noise Vibr Act Control* 2020; 39: 925-938. DOI: 10.1177/1461348419850921.
18. Bokaeian V, Rezvani MA and Arcos R. A numerical and scaled experimental study on ride comfort enhancement of a high-speed rail vehicle through optimizing traction rod stiffness. *J Vib Control* 2020; 27: 2548-2563.
19. Chen J, Wu Y, Zhang L, et al. Dynamic optimization design of the suspension parameters of car body-mounted equipment via analytical target cascading. *J Mech Sci Technol* 2020; 34: 1957-1969.
20. Fu B and Bruni S. An examination of alternative schemes for active and semi-active control of vertical car-body vibration to improve ride comfort. *Proc Inst Mech Eng, Part F: J Rail Rapid Transit* 2021. DOI: 10.1177/09544097211022108.
21. Huang C and Zeng J. Suppression of the flexible carbody resonance due to bogie instability by using a DVA suspended on the bogie frame. *Veh Syst Dyn* 2021: 1-20.
22. Nagai M, Yoshida H, Tohtake T, et al. Coupled vibration of passenger and lightweight car-body in consideration of human-body biomechanics. *Veh Syst Dyn* 2006; 44: 601-611.
23. Tomioka T and Takigami T. Experimental and numerical study on the effect due to passengers on flexural vibrations in railway vehicle carbodies. *J Sound Vib* 2015; 343: 1-19.
24. Tomioka T, Takigami T and Aida K. Experimental investigations on the damping effect due to passengers on flexural vibrations of railway vehicle carbody and basic studies on the mimicry of the effect with simple substitutions. *Veh Syst Dyn* 2017; 55: 995-1011.
25. Yu Y, Zhao L and Zhou C. A new vertical dynamic model for railway vehicle with passenger-train-track coupling vibration. *Proc Inst Mech Eng, Part K: J Multi-body Dyn* 2020; 234: 134-146.
26. Liao Y, Liu Y and Yang S. Semiactive Control of High-Speed Railway Vehicle Suspension Systems with Magnetorheological Dampers. *Shock Vib* 2019; 2019.
27. Iwnicki S. *Handbook of Railway Vehicle Dynamics*. 1st ed. New York: CRC press, 2006.

Appendix A

Table A.1. Physical and mechanical parameters of the Shinkansen high-speed vehicle[13].

Symbol	Description	Value	Unit
c_p	primary vertical damping coefficient (per axle)	78.4	kN.s.m^{-1}
c_s	secondary vertical damping coefficient (per bogie)	45.1	kN.s.m^{-1}
I_b	inertia moment for bogie frame pitching	2340	kg.m^2
I_c	inertia moment for carbody pitching	2.1×10^6	kg.m^2
k_p	primary vertical stiffness (per axle)	1.97	MN.m^{-1}
k_s	secondary vertical stiffness (per bogie)	2.65	MN.m^{-1}
k_{hz}	linearized stiffness of the Hertzian contact theory	1.504	MN.m^{-1}
l	carbody length	24.5	m
l_b	half the length of bogie-base	8.75	m
l_w	half the length of wheel-base	1.25	m

l_{pi}	the longitudinal position of the ith row of the passenger on the carbody from its rear end	-	m
m_c	carbody mass	16900	kg
m_b	bogie frame mass	2580	kg
m_w	wheelset mass	1510	kg
m_p	passenger mass	75	kg
ω_1	first mode frequency of the carbody bending	9.84	Hz
f_1	the natural frequency of passenger body-seat dynamic systems	-	Hz
ξ_1	first mode damping ratio of the carbody bending	0.012	-
η_1	the damping ratio of passenger body-seat dynamic system	-	-
v	vehicle running speed	300	$km.h^{-1}$